Available online at www.sciencedirect.com

ScienceDirect

Procedia Manufacturing 41 (2019) 531–538

Procedia MANUFACTURING

www.elsevier.com/locate/procedia

8th Manufacturing Engineering Society International Conference

Reinforced photocurable materials for an Additive Manufacturing process based on Mask Image Projection

J. Bonada[a,b,*], E. Xuriguera[c], A. Muguruza[a], J. Gonçalves[c], P. Barcelona[c], J.M. Pons[b], J. Minguella[a], R.Uceda[a]

[a]*Centre CIM, Llorens i artigas 12, Barcelona (08028), Spain*
[b]*Strength of Materials and Structural Engineering Department, Universitat Politècnica de Catalunya, Diagonal 647, Barcelona (08028) Spain*
[c]*Material Science and Physical Chemistry, Universitat de Barcelona, Martí i Franquès 1, Barcelona (08028), Spain*

Abstract

Mask Image Projection based on Stereolithography (MIP-SL) is an Additive Manufacturing (AM) system which it is based on a Frontal Photopolymerization Process (FPP) to manufacture parts made of photocurable materials. In this paper, a FPP numerical model is used to analyse the printability of different reinforced photocurable materials for MIP-SL manufacturing process. Consequently, optimal printing parameters could be defined to increase the material photoconversion ratio. Two different reinforcements are used to analyse the influence of fillers on FPP material coefficients. The results show the use of reinforcement could significantly enhance the mechanical properties obtained by means of experimental compression tests.

Keywords: Additive Manufacturing; Mask Image Projection; Mechanical properties; Reinforced Materials.

* Corresponding author. Tel.: +34-934016226.
E-mail address: jordi.bonada@upc.edu

© 2019 The Authors. Published by Elsevier B.V.
This is an open access article under the CC BY-NC-ND license (http://creativecommons.org/licenses/by-nc-nd/4.0/)
Peer-review under responsibility of the scientific committee of the 8th Manufacturing Engineering Society International Conference.

1. Introduction

Several Additive Manufacturing (AM) technologies use Frontal Photopolymerization Processes (FPP) [1,2] to obtain each material layer, such as Stereolithography (SLA) or Mask Image Projection based on Sterolithography (MIP-SL). MIP-SL, traditionally known as DLP (Digital Light Processing), commonly use a DMD (Digital Micro Device) system to emit a controlled light energy dose on a photocurable resin in order to built-up each layer. One of the advantages of MIP-SL is the simultaneously energy delivery in the whole manufacturing area; consequently, the manufacturing speed could be higher than traditional SLA. However, the manufacturing resolution of MIP-SL is limited by the number of pixels of the DLP projection system used.

In spite of FPP AM technologies could produce parts with higher resolution than other plastic 3D printing processes, the mechanical properties of photocurable resins are one of the main limitations of these manufacturing systems. In fact, it is known that some mechanical properties, such as Young's modulus, tensile strength, shrinkage or density, depend on the material photocuring conversion ratio [3,4]. Therefore, a right definition of printing parameters is a key factor to obtain a full homogenous conversion, as much as possible, in order to uniform the mechanical properties of printed parts. On the other hand, the addition of particles and fibres to reinforce photocurable resins to enhance their mechanical properties has been investigated [5-7]. Most of the existing research shows an increment of the Young Modulus through the addition of particles or fibres as main effect on the mechanical properties. However, the addition of particles also modifies the material viscosity and material attenuation factor and consequently could affect the FPP printing process. As a consequence, a right control of these parameters is necessary to ensure the printability of reinforced photocurable materials (suspensions).

The main goal of this paper is the analysis and evaluation of FPP parameters of photocurable materials according to the reinforcement used. In order to achieve this main objective, the FPP material parameters will be obtained through experimental tests measuring the thicknesses of different samples according to the energy dose emitted by the DLP projection system and FTIR analysis. Furthermore, numerical simulations based on FPP analytical models will be used to determine the printing parameters (mainly energy dose and layer thickness) which optimize the printing process in terms of photocuring conversion ratio. Other parameters to ensure the material printability such as sedimentation and viscosity will be taken into account. A preliminary evaluation of the elastic modulus of reinforced materials will be obtained by means of experimental compression tests.

2. Materials

An acrylic resin has been used as a photocurable material to obtain five different reinforced suspensions (Table 1) for a MIP-SL additive manufacturing process. Carbon fibres or alumina (Al_2O_3) particles, as a filler material, have been mixed into an acrylic resin (base material) in different solid load content (% in weight) to analyse its printability. The particle size of alumina and carbon fibres length are around 0.5 μm (D_{50}) and 200 μm, respectively.

Table 1. Characteristics of base and reinforced photocurable materials.

Material	Reinforcement	Solid Load (%w)
Base	None	-
CF2	Carbon Fibres	2%
CF4	Carbon Fibres	4%
A2.5	Al_2O_3 particles	2.5%
A5	Al_2O_3 particles	5%
A7.5	Al_2O_3 particles	7.5%

3. Frontal photopolymerization model

A photo-invariant analytical FPP model is used to describe the spatial-temporal monomer-to-polymer conversion ratio of photocurable materials [1-3]. Eq. 1 describes the conversion ratio by means of a dimensionless parameter (ϕ); where z is the manufacturing direction, μ the material attenuation factor, K is the material effective conversion rate and d the light energy exposure dose. When the conversion ratio is higher than a threshold value or gel point (ϕ_c) a network is formed and the material is solidified.

$$\phi = 1 - \exp\left(-K \cdot d \cdot \exp\left(-\mu \cdot z\right)\right) \tag{1}$$

The photo-invariant analytical model used assumes that the material attenuation factor and material effective conversion rate are independent of the material conversion ratio. Moreover, the oxygen inhibitory effect and the influence of thermal effects on the FPP kinetics have not been taken into account in this model.

Traditionally, in MIP-SL manufacturing process all mask images are projected with the same exposure energy dose (d_0). Consequently, the previous printed layers could receive and additional energy dose (Δd) for each new printed layer (Eq. 2) according to the material and printing parameters [4,8]. In fact, the first layers will receive a higher accumulated dose than the last ones. As a result, a stepped conversion ratio profile is commonly obtained as a consequence of layer thickness and material attenuation factor.

$$\Delta d = d_0 \exp\left(-\mu \cdot \Delta z\right) \tag{2}$$

A numerical model to predict the photoconversion ratio was developed and implemented in [8]. This model, based on a finite element discretization strategy, has been used to calculate the conversion ratio value of each spatial location of the manufacturing domain taking into account all projected mask images involved during the manufacturing process. Thus, the printing parameters to obtain a full conversion ratio of the photocurable material during the manufacturing process could be properly determined. In order to validate the numerical model in terms of conversion ratio, three samples with different exposure times have been manufactured and the conversion ratio values have been calculated through the numerical model and compared with experimental values obtained by means of FTIR analysis. The results (Fig. 1a) show a good agreement between numerical predictions and experimental measurements. Consequently, the numerical FPP model could be used to optimize printing parameters (exposure dose and layer thickness) to manufacture parts with higher and more uniform conversion ratio values and, as a result, with higher mechanical properties.

3.1. Calibration of photocurable material

The FPP parameters were obtained through experimental tests for each material defined at Section 2. A minimum of 5 samples were printed with a single mask image projected for each exposure doses of each material. The thicknesses of the samples (Z_f) depend on the energy dose. Thus, the material attenuation factor could be calculated as the inverse slope of the thickness – logarithmic dose relationship (Fig. 1b). It can be observed how the use of particles and fibres decreases the thickness of the samples as a consequence of a higher material attenuation factor.

On the other hand, the threshold conversion ratio value was obtained by means of FTIR spectrometry analysis of acrylate groups through the normalized peak area of the absorption band of 810 cm^{-1}. It has been considered that the threshold value remains constant. More details of the experimental calibration procedure can be consulted in [4,8].

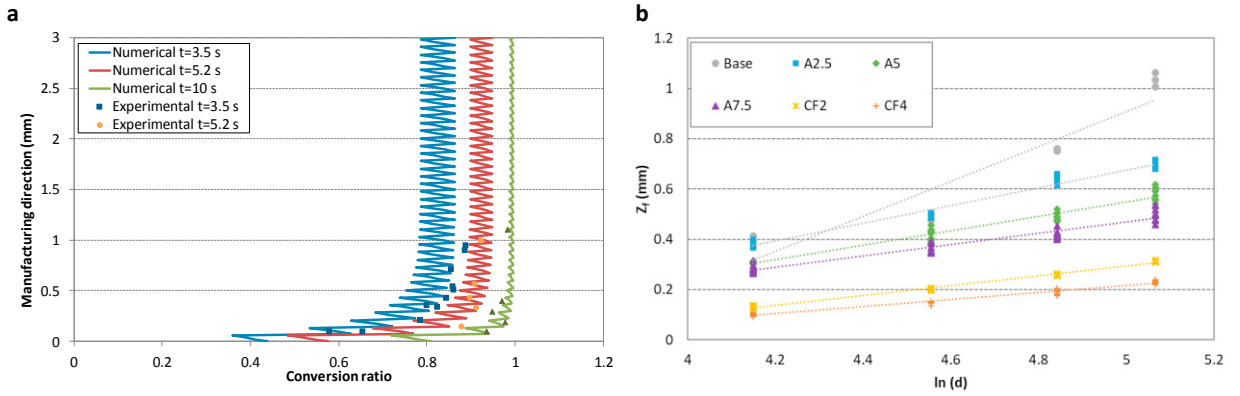

Fig. 1 (a) Numerical and experimental conversion ratio values along the manufacturing direction of samples with different exposure times; (b) Thicknesses of samples manufactured with a single image projected according to the logarithmic energy dose.

4. Influence of reinforcement particles into photocurable materials

4.1. Analysis of printability

The use of particles or fibres as fillers into a photocurable resin could change some FPP material parameters and modifies the material printability. First of all, the influence of material attenuation factor and material effective conversion rate parameters have been experimentally analysed. Fig. 2 shows the changes on these material parameters according to the type of reinforcement and solid load content. It can be observed that the addition of particles significantly increases the material attenuation factor of base material. The results also show the use of carbon fibres produces higher values of material attenuation factor than alumina particles. On the other hand, the material effective conversion rate value is also modified. However, the change of this parameter is lower than the attenuation factor.

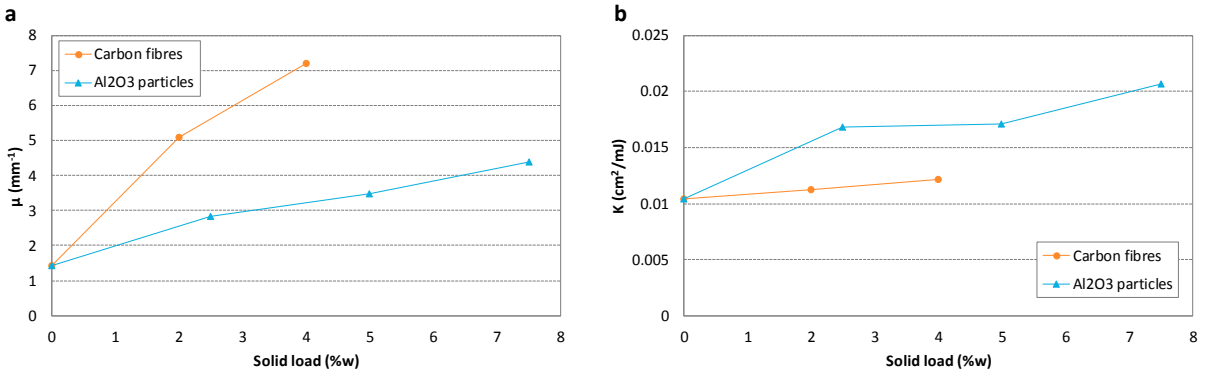

Fig. 2. (a) Variation of material attenuation factor; (b) Variation of material effective conversion rate.

One of the main parameters to evaluate the material printability is the minimum energy dose to obtain a successful printing process. This minimum dose (d_{min}) could be analytically calculated through Eq. 3, where Δz has been defined a 10% higher than the layer thickness in order to ensure a correctly bonded of each material layer. Fig. 3a shows the minimum energy dose required as a function of layer thickness for the base resin and reinforced suspensions. It can be observed that the minimum dose increases for a thicker layer. Furthermore, this effect is more notorious for materials with higher attenuation coefficient. The increase of this parameter could reduce the manufacturing speed and difficult the adhesion of the first layer on the construction platform.

$$d_{\min} = \frac{\exp(-\mu \cdot \Delta z) \cdot \ln\left(\frac{1}{1-\phi_c}\right)}{K} \tag{3}$$

The printing parameters could be adjusted to enhance the material conversion ratio and consequently improve mechanical properties. The conversion ratio of each spatial location depends on the total accumulated energy dose received taking into account all mask images projected during the whole manufacturing process. The conversion ratio at the top ($\phi_{AM\ Top}$) and bottom ($\phi_{AM\ Bottom}$) position of each layer can be calculated through Eq. 4 and 5, respectively, assuming that all printed layers are manufactured with the same energy dose. Therefore, the required energy dose to obtain a full conversion (d_{full}), which it has been defined as a minimum conversion ratio of 0.99 along the layer thickness, could be determined. The results are shown in Fig. 3b.

$$\phi_{AM\ \ Top} = 1 - \exp\left(-K \sum_{n=1}^{n^{o}layers} \left(d_{full} \cdot \exp\left(-\mu (n-1) \Delta z_{layer}\right)\right)\right) \tag{4}$$

$$\phi_{AM\ \ Bottom} = 1 - \exp\left(-K \sum_{n=1}^{n^{o}layers} \left(d_{full} \cdot \exp\left(-\mu \cdot n \cdot \Delta z_{layer}\right)\right)\right) \tag{5}$$

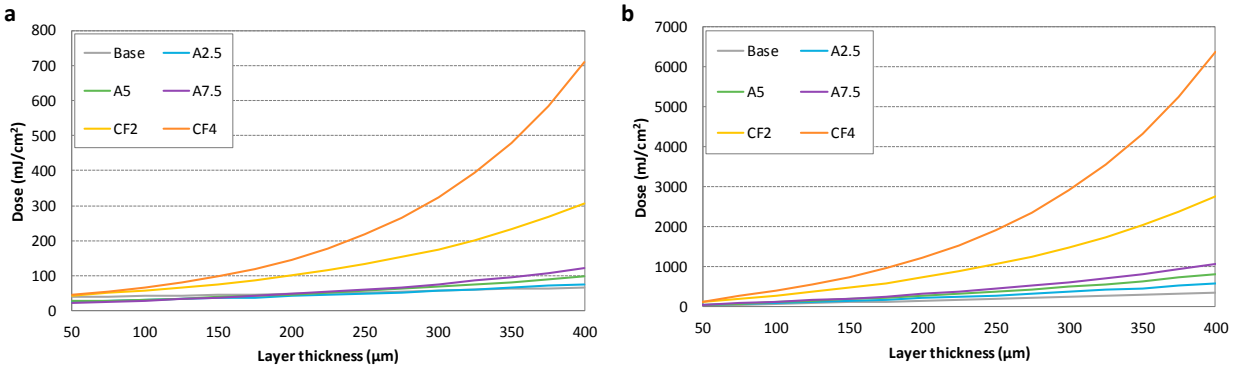

Fig. 3 (a) Minimum energy dose required to ensure the bonding between layers; (b) Energy dose for layer required to obtain a full material conversion ratio.

Although the use of the minimum energy dose is completely functional to built-up a 3D part, the conversion ratio value inside the manufactured part could be significantly lower than the maximum conversion achievable as it is shown in Fig. 4a. Furthermore, the conversion ratio gradient along each layer thickness is higher if the minimum energy dose is defined as a printing parameter. As a result, lower non-uniform mechanical properties along each layer thickness would be obtained. This effect is magnified in materials with a higher attenuation coefficient. A post-curing process in a UV oven is commonly used to increase the material conversion after the printing process to enhance mechanical properties. However, the post-curing treatment could only increase the material conversion inside a bulk manufactured part if the material attenuation factor is low; otherwise it would only increase the conversion ratio on the piece surface. Therefore, it is recommended to define properly printing parameters to obtain a full conversion ratio value during the manufacturing process.

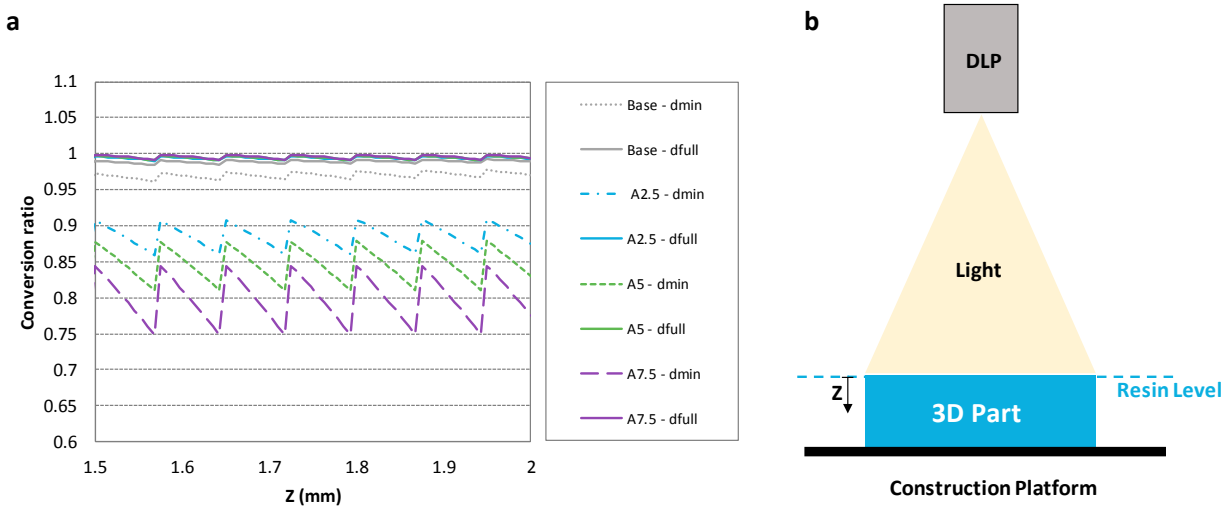

Fig. 4. (a) Conversion ratio value, after an initial number of layers, according to the energy dose and material (alumina suspensions) for a layer thickness of 75 µm; (b) MIP-SL top-down configuration.

Besides FPP parameters, low viscosity and sedimentation are other main characteristics to ensure the material printability. In all cases, the viscosity of the suspension is suitable to be printed in a MIP-SL equipment with a top-down configuration (Fig. 4b).

The suspensions with carbon fibres as a reinforcement show a high sedimentation rate. In fact, after 3 hours the sedimentation is clearly visible (Fig. 5a). Therefore, the formulation needs to be optimized in order to stabilize the suspension to obtain a homogenous printed part during the printing process. On the other hand, the material with alumina particles remains stable for 7 days, as it can be observed in Fig. 5b.

The use of carbon fibres produces a high increment of the material attenuation factor. Consequently, the exposure time of each mask image projected needs to be higher to reach a full conversion ratio value. Furthermore, a uniform distribution of carbon fibres cannot be properly assumed to print a compression coupon without using a mixer in the resin tank or optimizing the suspension formulation. Thus, the A5 material (alumina particles with a solid load content of 5% in weight) has been selected to make a preliminary evaluation of the influence of reinforcement on the mechanical properties of a photocurable resin in a MIP-SL AM process.

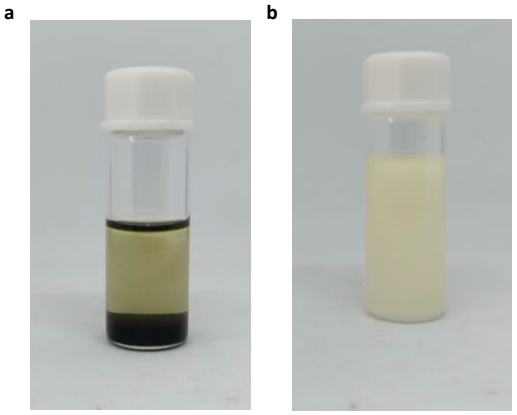

Fig. 5. (a) Carbon fibres sedimentation after 3 hours; (b) Suspension with alumina particles after 7 days.

4.2. Characteristics of MIP-SL equipment and printed samples

All printing parameters have been adjusted according to the MIP-SL equipment used to manufacture all compression coupons. A top-down configuration has been selected to avoid the effects caused by the detachment of the cured layers from the tank surface.

Compression coupons (base material and A5) have been printed with a layer thickness of 75 µm and a controlled temperature of 23ºC. A red dye has been mixed with the base material to increase the material attenuation factor to properly control the printing accuracy along the manufacturing direction; otherwise the low attenuation coefficient could produce non-desired solidification of material layers in non-desired parts as a consequence of the uncontrolled accumulated energy dose [8]. The exposure dose for both materials (base and A5) has been calculated through the FPP numerical model to obtain a full conversion ratio as it has been described in Section 4.1. All compression coupons have been manufactured with the same orientation on the construction platform (direction X defined in [9]).

4.3. Enhancement of mechanical properties

The compression mechanical properties of base and A5 (5% in weight of alumina particles) suspension have been obtained through experimental tests (4 different samples). All details about the experimental procedure could be found in [9]. The stress-strain behaviour of each sample is shown in Table 2 and Fig. 6. Finally, a statistical hypothesis testing of different elastic modules for the reinforced and base material has been done. The p-value obtained is 3.73e-5. Therefore, it could be assumed that the use of alumina particles, as a reinforcement, produces significant enhancement of mechanical properties

Table 2. Elastic modulus of reinforced (A5, 5% in weight of alumina particles) and base material.

Material	E (MPa)
A5 – Sample 1	554
A5 – Sample 2	577
A5 – Sample 3	593
A5 – Sample 4	529
A5 – Mean	**563**
Base – Mean	**206**

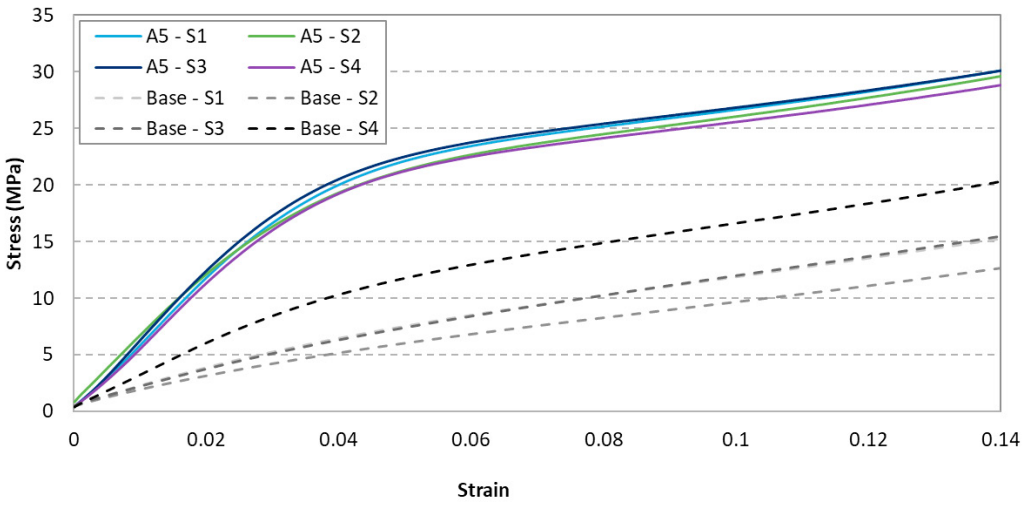

Fig. 6. Experimental stress-strain curves of reinforced (A5) and base material.

5. Conclusions

The results show the viability of using particles as a reinforcement on photcurable resins for MIP-SL Additive Manufacturing process. Moreover, a FPP analytical model could also be used to describe the polymer-to-monomer conversion of photocurable resins with reinforcement particles. First of all, the use of particles/fibres, as fillers, increase the material attenuation factor and also modifies the effective conversion rate. Therefore, the printing parameters need to be recalculated in order to print samples with a full conversion ratio. The attenuation coefficient is a key parameter to analyse the printability of photocurable materials. The increment of attenuation factor will increase the minimum energy dose to ensure the bonding of each material layer and also the required energy dose to obtain a full conversion after the printing process, which it is necessary requirement to achieve the maximum material mechanical properties. Consequently, the printability of the material could not be practical if the necessary exposure time to reach these energy doses is too high. Moreover, sedimentation is also another key factor to analyse the material printability. The sedimentation could be very different according to type, size, shape and solid load content used. The results show the viability of using alumina particles as reinforcement to manufacture parts with a homogenous reinforcement distribution.

Finally, the preliminary results of mechanical properties of reinforced materials show promising values. It can be observed an enhancement of elastic modulus and yield strength in compression tests. In following steps, the mechanical properties in tension tests will be obtained and compared with compression values. Furthermore, the variation of mechanical properties according to the solid load content of reinforcement will be analysed.

Acknowledgements

Authors (a), (b) and (c) would like to thank the Spanish Ministry of Economy and Competitiveness for financial support for the research project “Nuevas tecnologias para la impresion 3D de materiales avanzados” (DPI2016-80119-C3-1-R, DPI2016-80119-C3-2-R and DPI2016-80119-C3-3-R). The author J. Bonada is a Serra Húnter Fellow.

References

[1] J. Cabral, J. Douglas. Propagating waves of network formation induced by light. Polymer 2005; 30:4230-41.
[2] A. Vitale, J. Cabral. Frontal conversion and uniformity in 3D printing by photopolymerisation. Materials 2016; 9:760.
[3] A. Vitale, M.G. Henessy, O.K. Matar, J. Cabral. Interfacial profile and propagation of frontal photopolymerization waves. Macromolecules 2015; 48:198-205.
[4] J. Bonada, A. Muguruza, X. Fernández-Francos, X. Ramis. Influence of exposure tine on mechanical properties and photocuring conversion ratios for photosensitive materials used in additive manufacturing. Procedia Manufacturing 2017; 13: 762-769
[5] Z. Weng, Y. Zhou, W. Lin, T. Senthil, L. Wu. Structure-property relationship of nano enhanced stereolithography resin for desktop SLA 3D printer. Composites Part A: Applied Science and Manufacturing 2016; 88: 234-242.
[6] S. Kumar, M. Hofmann, B. Steinmann, E.J. Foster, C. Weder. Reinforcement of Stereolithographic resins for rapid prototyping with cellulose nanocrystals. ACS Appl Mater Interfaces 2012; 4(10): 5399–5407.
[7] H. Eng, S. Maleksaeedi, S. Yu, Y.Y.C Choong, F.E. Wiria, C.L.C. Tan, P.C. Su, J. Wei. 3D Stereolithgraphy of polymer composites reinforced with orientated nanoclay. Procedia Manufacturing 20017; 2016: 1-7
[8] J. Bonada, A. Muguruza, X. Fernández-Francos, X. Ramis. Optimisation procedure for additive manufacturing processes based on mask image projection to improve Z accuracy and resolution. Jounal of Manufacturing Processes 2018; 31: 689-702.
[9] M. Casafont, J.M. Pons, J. Bonada, M.M. Pastor, F. Marimon, F. Roure. Experimental study of the compression behavior of MIP-SL manufactured parts. Submitted to 8th Manufacturing Engineering Society International Conference.